AUT Journal of Electrical Engineering

AUT J. Elec. Eng., 51(2) (2019) 131-138
DOI: 10.22060/eej.2019.16260.5281

Highly Selective Lowpass Filter with Wide Stopband in Suspended Stripline Technology for Millimeter-wave Diplexer Applications

S. M. Miri[1], K. Mohammadpour-Aghdam[2*], S. O. Miri[3]

[1]PhD. Student, School of Electrical and Computer Engineering, University of Tehran, Tehran, Iran
[2]Assistant Professor, School of Electrical and Computer Engineering, University of Tehran, Tehran, Iran
[3]M.Sc., Alumnus of Electrical and Computer Engineering, Shiraz University, Shiraz, Iran

ABSTRACT: This paper presents a low loss and high selective lowpass filter which is implemented using suspended stripline (SSL) technology. The proposed structure is comprised of a 13th order generalized Chebyshev lowpass filter which enjoys integrated waveguide-to-SSL transitions. This filter is designed and fabricated to be used as lowpass channel of a U-band diplexer employed in frontend of a U-band down converter. Designed filter has cut-off frequency of 50 GHz with high performance out-of-band rejection and wide stopband associated with stepped-impedance resonators realized using generalized Chebyshev prototype. Final design of filter is analyzed and optimized using 3D full-wave simulator. Filter circuit is realized on one side of a 0.127 mm-thick TLY5 substrate with dielectric constant of 2.2, which is suspended symmetrically in a waveguide channel with height of 0.961 mm and maximum width of 2 mm. Higher order modes propagation effects on filter performance are investigated to have proper single mode operation. In addition, parametric study of SSL is done to predict probable malfunctioning due to misalignment or other fabrication and packaging errors. Measurement results also are presented to verify performance of filter. The filter displays a maximum passband insertion loss of 2 dB and a return loss of better than 10 dB over the passband. Band-edge steepness reaches over 50 dB at 5 GHz away from cut-off and out-of-band rejection is higher than 45 dB at entire stopband, which are in good agreement with simulation.

Review History:
Received: 2019-05-05
Revised: 2019-06-29
Accepted: 2019-07-09
Available Online: 2019-12-01

Keywords:
Lowpass filter
Suspended stripline
Generalized Chebyshev
Waveguide-to-SSL transition
U-band diplexer

1. Introduction

Nowadays, there is so much interest in millimeter-wave frequencies due to various features including higher data rates, less spectral crowding, and better spatial resolution. By development of integration technologies, millimeter-wave devices are used in many applications such as high data rate communication, transceivers, wireless systems, biomedical devices and imaging systems [1-3]. Since filtering circuits are mostly existing at frontend of transceivers, they have significant effects on system performance. To satisfy growing requirements of rapidly developing modern millimeter-wave communication systems, compact filters with low insertion loss, high selectivity, high stopband rejection, low cost and ease in fabrication and integration are in high demand.

To realize millimeter-wave filtering circuits with aforementioned characteristics, the suspended stripline (SSL) technology is known as a suitable transmission medium. In recent years, many microwave and millimeter-wave circuits such as power dividers, directional couplers, filters and multiplexers have been implemented using SSL technology. [4-6].

In comparison with other planar technologies such as microstrip, coplanar waveguide (CPW) and stripline, SSL has some notable advantages including low loss, less dispersion, wider frequency operation, flat group delay and better temperature stability. The cross-section of the typical configuration of SSL is shown in Fig. 1. It consists of a substrate suspended symmetrically between two ground planes. Since the dielectric substrate is much thinner rather than the height of the housing enclosure, electromagnetic fields are mostly confined to the air gaps between the substrate and ground planes. Hence, SSL has lower loss and its effective dielectric constant will be made close to unity so that the dominant propagation mode will be quasi-TEM causing wider frequency range of operation with less dispersion. Besides, a small change in dielectric constant which can be due to temperature variations, has a small impact on the propagation characteristics. Therefore, SSL has better temperature stability. In addition, both sides of substrate can be used for making circuit pattern in SSL providing strong coupling for realization of wideband filters with small circuit size.

SSL has been extensively used in a variety of microwave and millimeter-wave filter designs [7-9]. In [10], a SSL bandpass filter with fractional bandwidth of 160% centered at 10 GHz was realized using cascaded generalized Chebyshev lowpass and pseudo-highpass filters. Also in [11, 12] two filters with finite frequency transmission zeros were proposed

*Corresponding author's email: kaghdam@ut.ac.ir

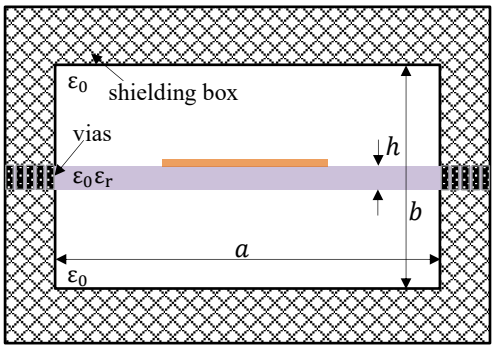

Fig. 1. Cross-section of SSL structure

Table 1. Design specifications

Parameter	Value (dB)	Frequency Range (GHz)
Return Loss	≥ 10	DC-50
In-band Insersion Loss	≤ 2	DC-50
Rejection	≥ 50	At 5 GHz from band-edge

for enhancing band-edge steepness and improving out-of-band rejection performance. Also some contiguous diplexers, implemented using combination of broadband SSL lowpass and highpass filters, were proposed in [13, 14].

This paper focuses on design of a 13th order generalized Chebyshev lowpass filter to be used as lowpass channel of a U-band diplexer existing in frontend of a U-band integrated down converter. The filter pattern is implemented on 0.127 mm-thick TLY5 substrate with dielectric constant of 2.2 and loss tangent of 0.009 which is suspended symmetrically in a metal waveguide channel with maximum width of 2 mm and 0.961 mm height. WR19 waveguide-to-SSL transitions at filter ports are used to integrate the proposed filter in frontend of a millimeter-wave down converter. The full-wave simulation is further used to validate the filter response. In section 3, fabricated filter is shown and measurement results are provided. Then, section 4 points to the application of proposed filter. Finally, conclusion are also given in section 5.

2. Design and Simulation

Herein, we need a wideband and high selective lowpass filter to be used in a contiguous diplexer with design specifications which are described in Table 1.

The proposed parameters are necessary to satisfy high selectivity and wide bandwidth requirements of the lowpass channel of millimeter-wave diplexer. The elliptic function prototype is realized with minimum possible degree for a given selectivity and passband ripple. Due to adjustable transmission zeros at desirable finite frequency, selectivity of generalized Chebyshev prototype is better than conventional Chebyshev while it is very close to that of elliptic prototype with the same degree. Furthermore, generalized Chebyshev prototype requires impedance variations of up to 2:1 versus 10:1 of an elliptic prototype. Due to implementation considerations of printed circuit board (PCB) technology, realization of such various impedance values of elliptic function prototype is extremely difficult and generalized Chebyshev is a more suitable and practical solution [15].

When operating in the millimeter-wave frequency bands and with regard to the filter characteristics, mode propagation and undesirable resonances within the enclosure are important concerns because they can cause spurious response so that they may affect the rejection characteristics of the filter. So, it is required to keep the width of cavity narrow to avoid exciting higher order modes within the cavity. Therefore, the cut-off frequency of the dominant TE_{10} waveguide mode should be set to be above 75 GHz to prevent degradation of the filter performance in operation frequency band. The cut-off frequency can be calculated from the following equation [14]:

$$f_c = \frac{c}{2a}\sqrt{1-\frac{h}{b}\left(\frac{\varepsilon_r - 1}{\varepsilon_r}\right)} \quad (1)$$

where a and b are the width and the height of channel respectively, c is the speed of light, h is the substrate height, and ε_r is the relative permittivity of the substrate.

Also, the height of cavity must be smaller than $\lambda/4$ at maximum operation frequency to prevent happening box resonances at high frequencies.

2-1- Filter Design

To design lowpass filter with cut-off frequency of 50 GHz with passband ripple of 0.1 dB and specifications mentioned in Table 1, generalized Chebyshev lowpass is more preferred because it can achieve high selectivity due to transmission zeros at order $(N-1)$ at a finite frequency, ω_0, near to band-edge and a single zero at infinity. With regarding to required rejection level at desirable distance from the band-edge, filter degree is chosen equal to 13 using design chart for generalized Chebyshev filter given in [16].

Rhodes in [16] presented generalized Chebyshev characteristics as well as the element values of lowpass prototype for different filter degrees according with desirable input return loss and rejection levels.

As shown in Fig. 1, the filter pattern should be implemented on one side of substrate. For physical realization, the lumped element generalized Chebyshev lowpass prototype is transformed into distributed model by applying Richard's transformation [15]. This filter is implemented using series $\lambda/8$ short circuit high impedance and shunt open circuit $\lambda/4$ as low impedance transmission lines at frequency of first transmission zero.

According to the equations of characteristic impedance and normalized static capacitance of SSL, mentioned in [17], by assuming strip thickness as zero for a printed circuit and effective dielectric constant near to one due to SSL, the width of metal strip can be calculated as equation below:

$$w = \frac{b}{4}\left(\frac{\eta_0}{Z_0} - 1.84\right) \quad (2)$$

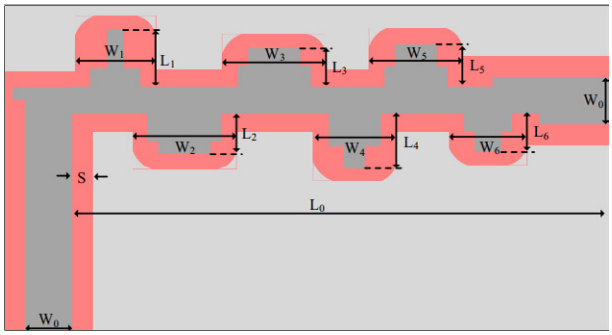

Fig. 2. 2D layout of lowpass filter

Table 2. Dimensions for lowpass filter

Parameter	Value (mm)	Parameter	Value (mm)	Parameter	Value (mm)
W_1	1.55	W_6	1.5	L_4	1.06
W_2	2	W_0	0.9	L_5	0.85
W_3	2	L_1	1.1	L_6	0.73
W_4	1.6	L_2	0.8	L_0	11.85
W_5	1.8	L_3	0.76	S	0.3

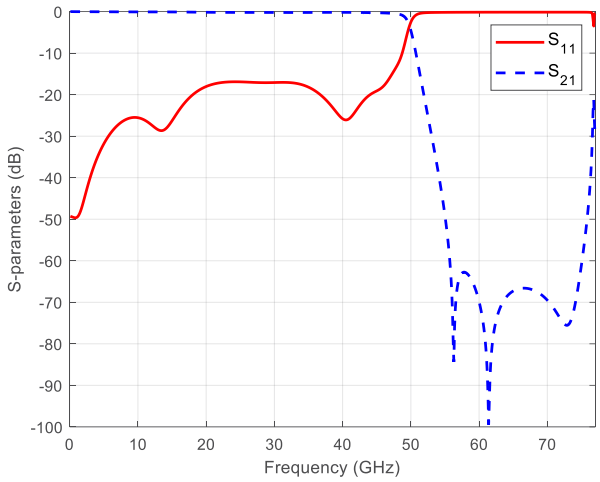

Fig. 3. S-parameter simulation results of single lowpass filter

where b is the height of cavity in mm, η_0 is free space characteristic impedance and Z_0 is the characteristic impedance of transmission line.

2-2- Waveguide-to-Suspended Stripline Transition

In order to measure the characteristics of proposed millimeter-wave filter, two waveguide-to-suspended stripline transitions are necessary to be integrated with the filter ports. This filter finally will be used in a contiguous U-band diplexer. So, the frequency response of filter can be measured in U band by using U-band 1.85 mm coaxial to waveguide adaptors.

The transition should have acceptable impedance matching and mode conversion between waveguide and SSL. Therefore, a broadside probe-type transition is selected. The probe is an extension of suspended stripline into the waveguide so that the probe surface faces the direction of propagation of the

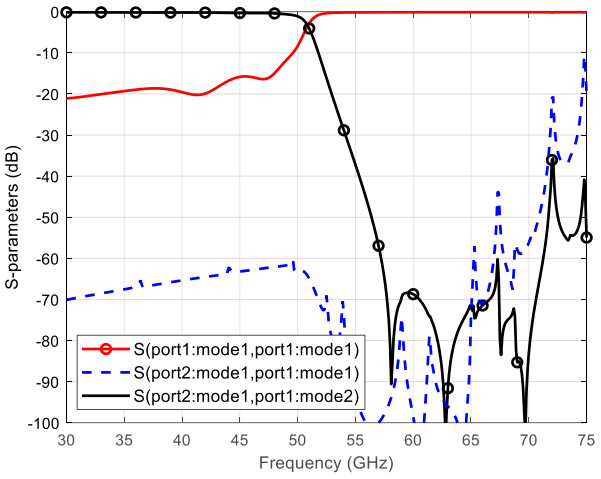

(a)

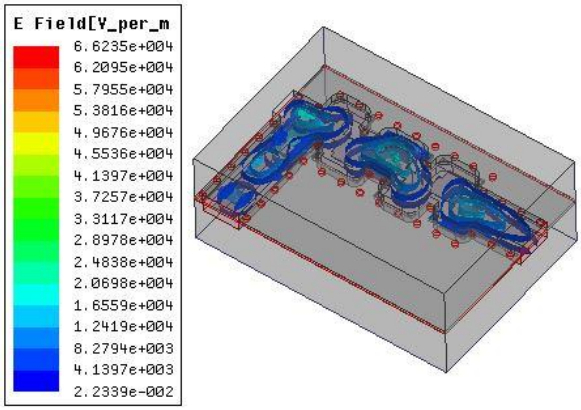

(b)

Fig. 4. Higher order modes propagation effects for 500um spacing (a) S-parameters showing resonances in rejection band (b) electric field distribution at 72.1 GHz showing higher order mode propagation

waveguide. Probe shape and insertion distance of suspended stripline into the waveguide are critical parameters to ensure that maximum energy is coupled from TE_{10} dominant mode in waveguide to quasi-TEM mode in SSL. Also the distance between the probe and the back-short is determined equal to one quarter of guide wavelength, $\lambda_g/4$, to change the phase of the opposite propagating wave by 180 degrees and add it to direct propagation wave in similar phase. So maximum energy flows in the direction of propagation and optimum matching is provided.

2-3- Simulation

The lowpass filter is analyzed using 3D full-wave simulator. 2D layout representation of the distributed lowpass filter is shown in Fig. 2 and associated distributed circuit parameters are provided in Table 2 after final optimization. The different length of shunt stubs of the SSL filter, causing different resonant frequencies, ensures that the stopband extends to the highest resonant frequency of shortest stub and hence, wider stopband can be achieved in this way. Simulation results for S-parameters of the proposed filter are depicted in Fig. 3. The

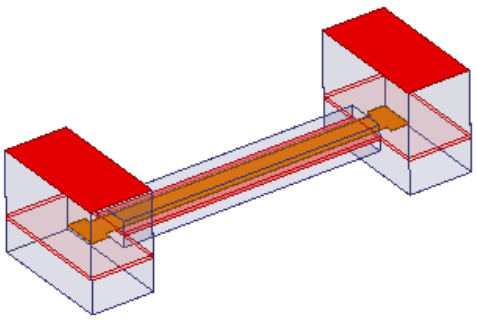

Fig. 5. Back to back WR19 waveguide-to-SSL transition

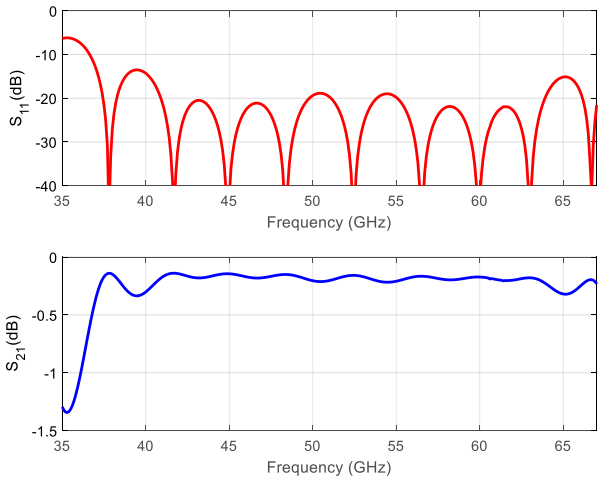

Fig. 6. S-parameter simulation results of back to back transition

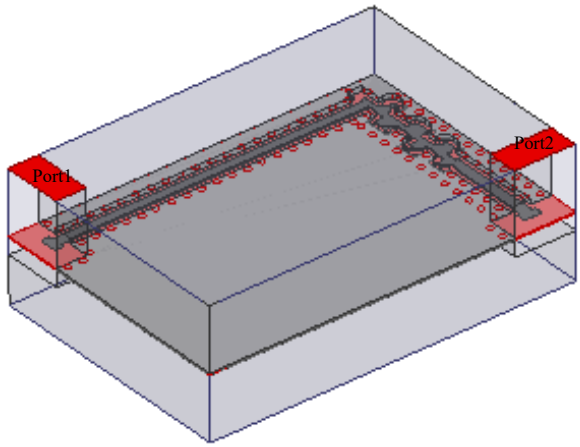

Fig. 7. 3D view of designed LPF

filter response shows the return loss, better than 10 dB, up to 50 GHz with very low insertion loss in the passband. Also the filter has a wideband rejection of higher than 60 dB except within 12% of band-edge frequency and sharp rejection such that insertion loss falls away below -50 dB at 5 GHz from the band-edge.

As mentioned in Table 2, the spacing between strip edge and box border has been chosen equal to 300um, to avoid high order modes excitation up to 75 GHz. Indeed, when

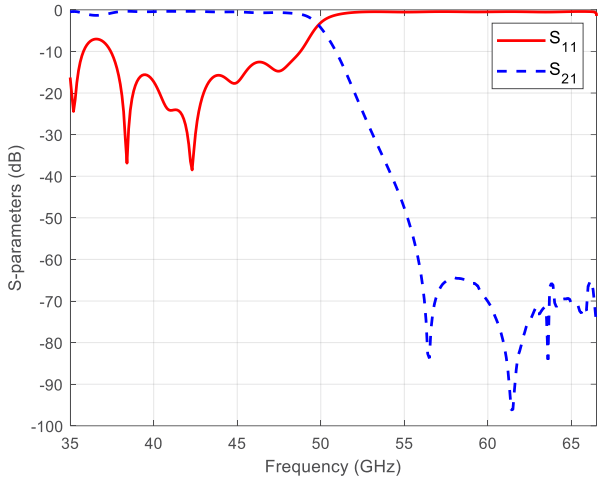

Fig. 8. S-parameter simulation results of designed LPF

this spacing is increased, high order modes will propagate and affect rejection characteristics of the filter, as shown in Fig. 4 which demonstrates the filter response for 500um spacing. In Fig. 4(a), several resonance frequency points can be recognized in rejection band of filter (specifically at 65, 67, 72.1 and 75 GHz), which caused by excitation of high order modes. Fig. 4(b) also demonstrates electric field distribution of high order modes in filter at 72.1 GHz. Therefore, the spacing and consequently width of channel should be determined somehow to have proper single mode operation in desirable frequency band.

Based on the described approach, an optimal transition is designed as illustrated in Fig. 5. The simulation results of designed back to back transition are presented in Fig. 6. The return loss is better than 15 dB in frequency range of 37-67 GHz with very low insertion loss in the passband.

To complete the filter structure, designed waveguide-to-SSL transition is connected to single lowpass filter as shown in Fig. 7. Since two U-band coaxial to waveguide adaptors are required to evaluate the filter performance and also to ensure that the waveguide modes will not propagate in desirable operation frequency band, the input and output transmission line sections of filter are extended with respect to adaptor dimensions. However, high rejection of designed filter also suppresses higher order waveguide modes at the input and output ports of filter. The simulation results of entire filter structure are shown in Fig. 8. The return loss is better than 10 dB in the entire bandwidth of 40-50 GHz. Also the filter has a wideband rejection of higher than 60 dB except 12% of band-edge frequency and sharp band-edge roll-off such that the insertion loss falls away below -50 dB at 5 GHz from the band-edge.

Electric field pattern for optimized design of filter at frequencies of 40 GHz, as passband, and 60 GHz , as stopband, are shown in Fig. 9(a) and Fig. 9(b). This Figure shows how filter passes or rejects input signal at passband frequency of 40 GHz and frequency of 60 GHz respectively.

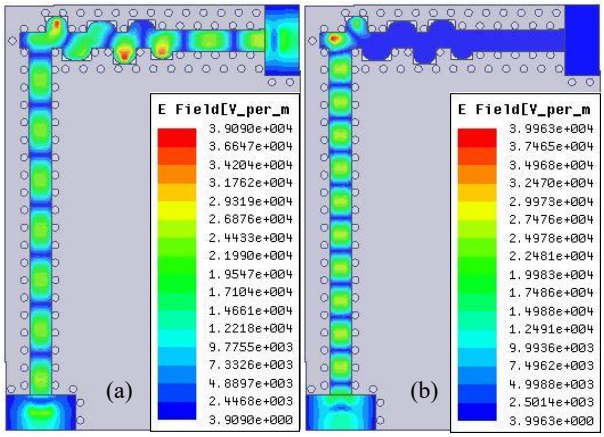

Fig. 9. Electric field pattern (a) at 40 GHz passing input signal (b) at 60 GHz rejecting input signal

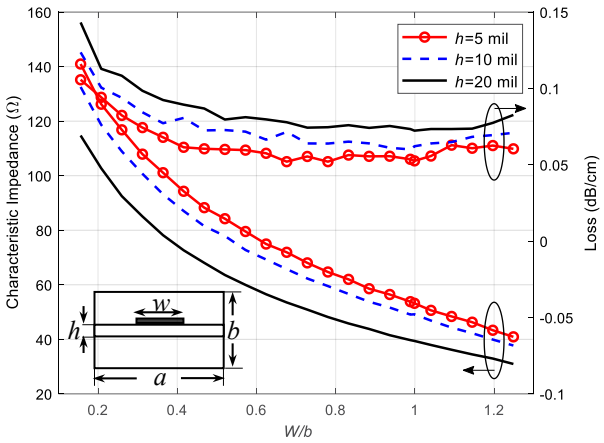

Fig. 10. Characteristic impedance and insertion loss of SSL versus *w/b* at 50 GHz for three different thicknesses of substrate with *b*=0.961 mm, *a*=1.5 mm.

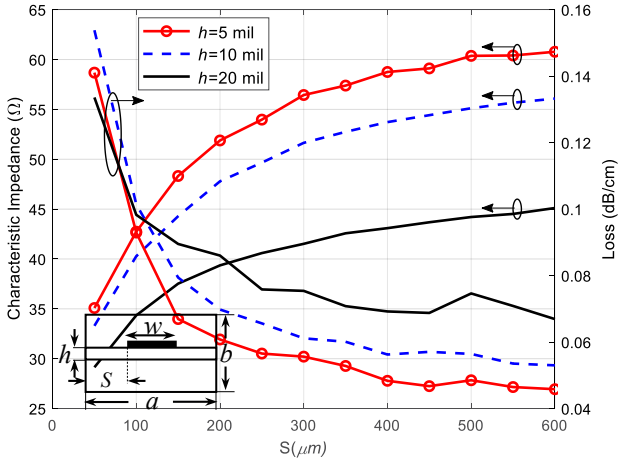

Fig. 11. Characteristic impedance and insertion loss of SSL versus *S* at 50 GHz for substrates of various thicknesses with *b*=0.961 mm, *w*=0.9 mm.

2-4- Parameter Study of Suspended Stripline

In the fabrication process, any offset in alignment of suspended stripline or etching error in PCB process or box fabrication, may destroy the filter response. So, sensitivity analysis is very important. Herein, analysis is carried out by changing strip width, spacing and offset caused by possible misalignment.

The variations in characteristic impedance and insertion loss of SSL as a function of strip width over cavity height, *w/b*, for three different thicknesses of substrate are depicted in Fig. 10. It is observed that for a fixed value of *w/b*, characteristic impedance, *Z*, decreases and loss increases with an increase in thickness of substrate, *h*, whereas, for a fixed value of *h*, both *Z* and loss decrease with an increase in *w/b*. However, small variations can be seen in insertion loss with *w* changing.

The simulation results of characteristic impedance and insertion loss of SSL for different spacing between metal strip and box border are demonstrated in Fig. 11 for substrates of various thicknesses. When spacing, *S*, is increased for a fixed value of *h*, value of *Z* increases but loss decreases. Also, for a fixed value of *S*, *Z* decreases and loss increases as *h* is increased.

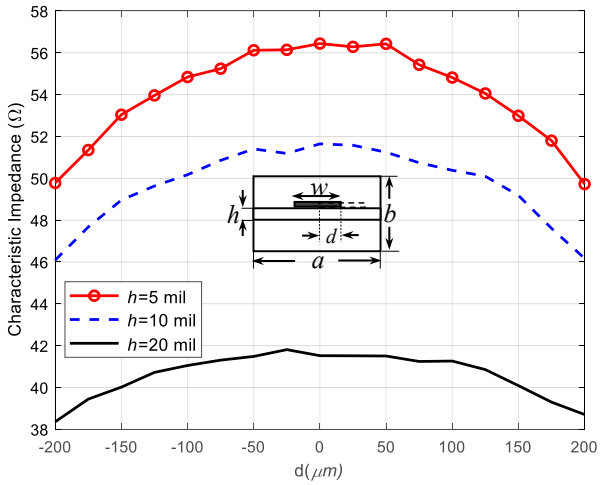

Fig. 12. Characteristic impedance of SSL versus offset *d* at 50 GHz for substrates of various thicknesses with *b*=0.961 mm, *a*=0.9 mm, *w*=0.9 mm.

Fig. 12 describes the variation of characteristic impedance as a function of offset between center of strip and center of channel width for different thicknesses of substrate. One can see as the offset is increased; the characteristic impedance decreases. Also, for lower thickness of substrate, more variations in *Z* can be seen.

As seen, characteristic impedance and insertion loss of SSL vary with metal strip width, spacing and offset between center lines of strip and channel. So, almost high precision fabrication and packaging processes, with at least 50um fabrication error, are required to have a wideband SSL filter with suitable performance at millimeter-wave frequencies because any considerable etching error or misalignment during packaging may lead to malfunctioning.

3. Fabrication and Measurement

Fig. 13(a) illustrates a module consisting designed lowpass

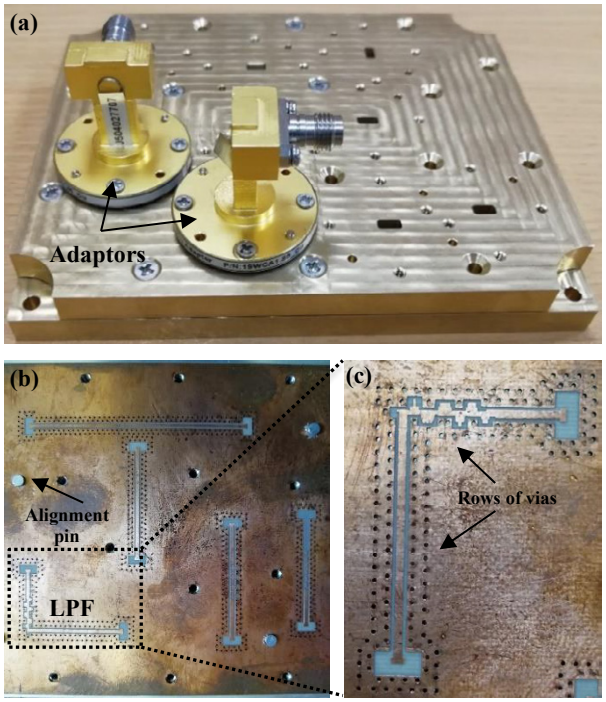

Fig. 13. (a) Integrated module connecting to 1.85 mm coaxial waveguide to WR19 adaptors (b) Printed circuit board of integrated module consisting designed lowpass filter (c) Printed circuit of SSL lowpass filter

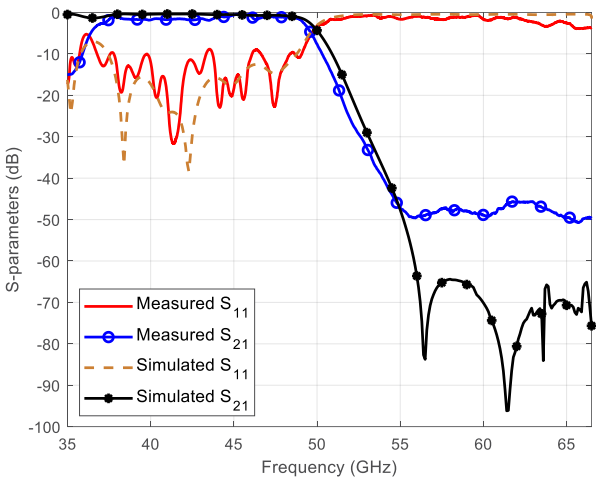

Fig. 14. S-parameter measurement results of fabricated filter

filter structure connected to 1.85 mm coaxial to WR19 waveguide adaptors with its alignment pins and screws. The alignment pins provide accurate positioning of the suspended stripline in waveguide cavity of the filter. In addition to proposed filter, some other SSL transmission lines and filters have been integrated on the same board as shown in Fig. 13(b). Transmission lines will be used in other works for insertion loss evaluation and filters will be applied in implementation of a U-band diplexer.

The air cavities are realized by using milling into two pieces of brass rectangular box. The printed board of filter is

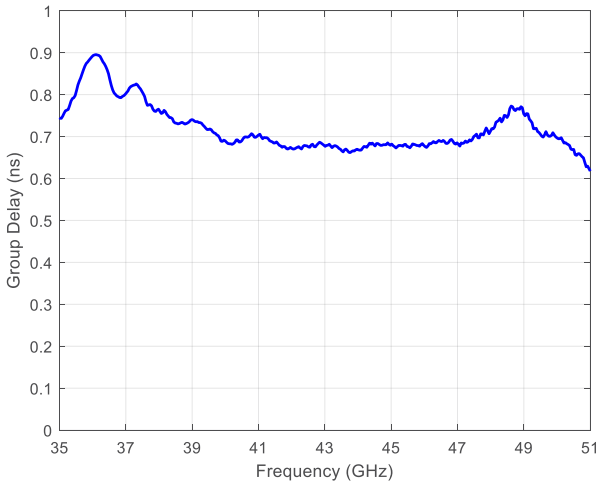

Fig. 15. Measured group delay response from 35 GHz to 51 GHz of lowpass filter

sandwiched between top and bottom halves of housing. These parts are brought together with prepared screws. Two parts of metal housing is electrically connected by the rows of vias along the edges of filter channel as can be seen in Fig. 13(c).

For S-parameter measurement, U-band 1.85 mm coaxial to waveguide adaptors are added to the filter structure. An Agilent vector network analyzer (VNA) is used for measuring the filter response. Before measuring the S-parameters of filter structure, the through connection was formed by connecting two adaptors directly back to back. By measuring the S-parameters of this back to back configuration, the filter response from output of adaptors as reference planes can be determined. Fig. 14 shows the measured S-parameters of the proposed filter from defined reference planes. The results indicate that the return loss is better than 10 dB at entire bandwidth. The passband insertion loss is better than 2 dB. Measured results also show a wideband and high rejection response so that 50 dB roll-off point is 5 GHz away from the band-edge and rejection is higher than 45 dB at entire stopband of filter.

Group delay is a useful measure of signal distortion, and is calculated by differentiating, with respect to frequency, the phase response of the device under test. So, we measured and recorded magnitude and phase of S_{21} and calculated group delay of filter using a MATLAB code. Fig. 15 displays the measured group delay of lowpass filter and is reported to be better than 700 picoseconds with good flatness between 40 GHz and 50 GHz except near to the band-edge. Slight peaking in group delay around the band-edge region from 48 GHz to 50 GHz is due to abrupt phase variation when transitioning from passband to rejection band. Indeed, transmission zeros located at a frequency near to the band-edge cause phase change of filter response in nonlinear form leading to non-flat group delay near to the band-edge. The deviation in group delay from the band-edge frequency at 49.9 GHz to mid-band at 45 GHz is less than 20 picoseconds. Also, the peaking in group delay from 35 GHz to 39 GHz is mainly due

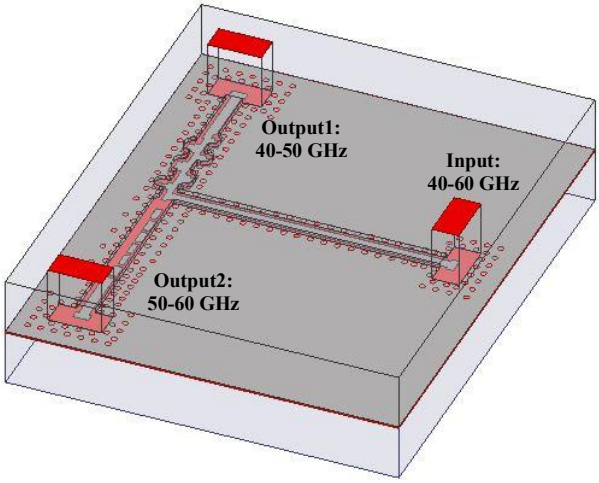

Fig. 16. U-band diplexer realized by shunting lowpass and pseudo-highpass filters with crossover at 50 GHz

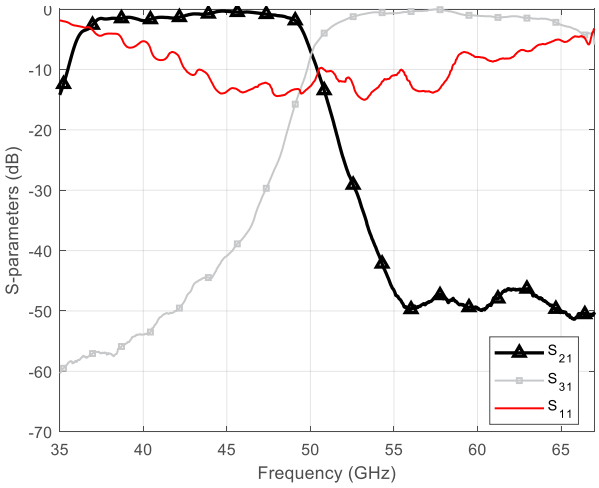

Fig. 17. S-parameters of U-band diplexer

to rapid phase variation when transitioning from TE_{10} mode of nonplanar waveguide to quasi-TEM mode of planar SSL filter.

The shift in cut-off frequency and differences in rejection of stopband in comparison with simulation results are mainly because of fabrication errors such as the etching tolerance of metal box and PCB.

4. Application

The proposed filter is a building part of a U-band diplexer, which will be used as input terminal and lowpass channel of diplexer. This diplexer, as shown in Fig. 16, comprises of a lowpass filter connected in parallel with a pseudo-highpass filter realized with broadside-coupled half-wavelength resonators. Measured S-parameters of diplexer are shown in Fig. 17 in which lowpass channel response is highlighted. As seen, designed diplexer has two channels with high selectivity and wide out-of-band rejection. Design and implementation of this diplexer will be presented in another work.

5. Conclusion

Based on a 13th order generalized Chebyshev lowpass prototype, a wideband and high rejection SSL lowpass filter with cut-off frequency of 50 GHz has been implemented using 0.127 mm-thick TLY5 substrate. The filter is combined of a single lowpass filter and two U-band WR19 waveguide-to-SSL transitions at filter ports allowing integration in frontend of a U-band down converter as lowpass channel of a diplexer. The filter exhibits the return loss better than 10 dB for the majority of frequency band as well as passband insertion loss below 2 dB. Due to transmission zeros at finite frequency near the band-edge, the filter has a good selectivity so that measured results show rejection higher than 45 dB at entire stopband with 50 dB roll-off point at 5 GHz away from the band-edge. Also sensivity analysis has been carried out by changing strip width, spacing and offset to consider malfunctioning caused by possible misalignment. In spite of small differences between simulation and measurement results due to fabrication errors, good correlation between them has been realized.

English symbols

a	Channel width, mm
b	Channel height, mm
c	Light speed in free space, m/s
d	Offset between center lines of strip and channel width, mm
h	Substrate height, mm
N	Degree of filter
S	Spacing between strip edge and box border, mm
w	Strip width, mm
Z	Characteristic Impedance, Ω

Greek symbols

λ_g	Guided wavelength, mm
ε_r	Relative permittivity
η_0	Free space characteristic impedance, Ω
ω_0	Transmission zero frequency, rad/m

Superscript

*	Corresponding Author

References

[1] B. Rupakula, A. Nafe, S. Zihir, Y. Wang, T.-W. Lin, G. Rebeiz, 63.5–65.5-GHz Transmit/Receive Phased-Array Communication Link With 0.5–2 Gb/s at 100–800 m and±50 Scan Angles, IEEE Transactions on Microwave Theory and Techniques, 66(9) (2018) 4108-4120.

[2] M.J. Horst, M.T. Ghasr, R. Zoughi, Design of a Compact V-Band Transceiver and Antenna for Millimeter-Wave Imaging Systems, IEEE Transactions on Instrumentation and Measurement, 68(11) (2019) 4400-4411.

[3] A. Mirbeik-Sabzevari, S. Li, E. Garay, H.-T. Nguyen, H. Wang, N. Tavassolian, Synthetic ultra-high-resolution millimeter-wave imaging for skin cancer detection, IEEE Transactions on Biomedical Engineering, 66(1) (2018) 61-71.

[4] A.F. Elshafey, M.A. Abdalla, Low Loss High Power Air Suspended Stripline Power Divider for High Power Division Sub-Systems Applications, Progress In Electromagnetics Research, 73 (2018) 153-162.

[5] J. Sorocki, I. Piekarz, S. Gruszczynski, K. Wincza, J. Papapolymerou, Application of 3D Printing Technology for the Realization of High-

Performance Directional Couplers in Suspended Stripline Technique, IEEE Transactions on Components, Packaging and Manufacturing Technology, 9(8) (2019) 1652-1658.
[6] N.B.M. Najib, N. Somjit, I. Hunter, Design and characterisation of dual-mode suspended-substrate stripline filter, IET Microwaves, Antennas & Propagation, 12(9) (2018) 1526-1531.
[7] L. Song, B. Wu, L. Xia, Y. Guo, J. Chen, T. Su, Compact tunable cavity filter with high selectivity using double-layer suspended stripline resonator, Microwave and Optical Technology Letters, 61(5) (2019) 1177-1180.
[8] M. Assaf, A. Malki, A.A. Sarhan, Synthesis and Design of MMR-Based Ultra-Wideband (UWB) Band Pass Filter (BPF) in Suspended Stripline (SSL) Technology, Progress In Electromagnetics Research, 84 (2019) 123-130.
[9] Z. Xu, Y. Hu, Y.P. Chen, K. Kang, J. Le Wei Li, A suspended stripline bandpass filter using hybrid transmission line stepped impedance resonator, Microwave and optical technology letters, 58(4) (2016) 892-895.
[10] J. McDaniel, J.B. Yan, P. Gogineni, Super-wideband cascaded bandpass filter using suspended substrate stripline technology, Microwave and Optical Technology Letters, 61(6) (2019) 1491-1499.
[11] Z.-X. Xu, X. Yu, J.-Q. Liu, O.K. KS, J.L.-W. Li, Suspended stripline UWB bandpass filter with adjustable transmission zero, in: 2014 Asia-Pacific Microwave Conference, IEEE, 2014, pp. 929-931.
[12] M.H. Ho, W. Hong, L.J. Lin, Low-pass filter of suspended stripline design with finite transmission zeros for stop-band rejection improvement, Microwave and Optical Technology Letters, 56(2) (2014) 297-301.
[13] I. Ashiq, A. Khanna, Ultra-broadband contiguous planar DC-35–65 GHz diplexer using softboard suspended stripline technology, in: 2013 IEEE MTT-S International Microwave Symposium Digest (MTT), IEEE, 2013, pp. 1-4.
[14] I. Ashiq, A. Khanna, A novel planar contiguous diplexer DC-67-100 GHz using Organic Liquid Crystal Polymer (LCP), in: 2015 IEEE MTT-S International Microwave Symposium, IEEE, 2015, pp. 1-4.
[15] S.A. Alseyab, A novel class of generalized Chebyshev low-pass prototype for suspended substrate stripline filters, IEEE Transactions on Microwave Theory and Techniques, 30(9) (1982) 1341-1347.
[16] J.D. Rhodes, S. Alseyab, The generalized chebyshev low-pass prototype filter, International Journal of Circuit Theory and Applications, 8(2) (1980) 113-125.
[17] S.M. Miri, K. Mohammadpour-Aghdam, S.O. Miri, A Millimeter-wave High Selective Lowpass Filter in Suspended Stripline Technology, in: 2018 Fifth International Conference on Millimeter-Wave and Terahertz Technologies (MMWaTT), IEEE, 2018, pp. 12-15.

HOW TO CITE THIS ARTICLE

S.M. Miri, K. Mohammadpour-Aghdam, S.O. Miri, Highly Selective Lowpass Filter with Wide Stopband in Suspended Stripline Technology for Millimeter-wave Diplexer Applications, AUT J. Elec. Eng., 51(2) (2019) 131-138.

DOI: 10.22060/eej.2019.16260.5281